Correlation of Zero Field Splittings and Site Distortions III. $MnBr_4^{2-}$ and Crystal Structure Refinements for Rb_3ZnBr_5 and Cs_2ZnBr_4

M. Heming and G. Lehmann
Institut für Physikalische Chemie, Westfälische Wilhems-Universität, Münster

and G. Henkel and B. Krebs
Institut für Anorganische Chemie, Westfälische Wilhelms-Universität, Münster

Z. Naturforsch. **36a**, 286–293 (1981); received January 31, 1980

EPR data for Mn^{2+} in Cs_2ZnBr_4, Rb_3ZnBr_5, Cs_3CdBr_5 and $[(CH_3)_4N]_2ZnBr_4$ single crystals were determined and the crystal structures of Rb_3ZnBr_5 and Cs_2ZnBr_4 were refined. Superposition analysis of the fine structure data for the latter two compounds resulted in an intrinsic zero field splitting parameter $\overline{b_2}$ for $MnBr_4^{2-}$ of $+0.44$ cm^{-1} suggesting a sizeable positive contribution of covalency. Cs_3CdBr_5 was prepared in single crystals for the first time. It crystallizes in a primitive tetragonal space group. From the fine structure parameter b_2^0 and the above value of $\overline{b_2}$ an elongation of the $CdBr_4^{2-}$ tetrahedra along the c-axis with a bond angle of 105.7° was determined. This result is in agreement with the anisotropy of the ^{55}Mn hyperfine splitting constant with $A_\parallel = -68.6$ and $A_\perp = -70.6 \cdot 10^{-4}$ cm^{-1}.

Introduction

The zero field splittings of S-state ions are — at least for their largest part — determined by the distortions of their first coordination spheres. Growing though not yet generally accepted evidence for this statement stems from quantitative correlations of sign and size of the second order axial splitting parameter b_2^0 with deviations of bond angles [1] and bond lengths [2] from cubic symmetry, from evaluation of uniaxial strain data for Mn^{2+} and Fe^{3+} in MgO and CaO [3] and from various applications [4–6] of the superposition model of Newman [7]. With a very large body of available EPR data such correlations are in most cases limited by the accuracy of the necessary crystal structure data (if complete parameter sets are at all available). For Fe^{3+} the sign of b_2^0 is also still unknown in many cases. Almost completely unknown is the dependence of the intrinsic zero field splitting parameter $\overline{b_2}$ [7] on the type of ligand, since the available data are restricted to a few ligands only.

As part of a systematic study, EPR data for $MnBr_4^{2-}$ in single crystals of four compounds were evaluated. The results for two of these were subjected to a superposition analysis using the results of simultaneous crystal structure refinements for these compounds. The resulting value of $\overline{b_2}$ allowed for the determination of the distortion angle of the $CdBr_4^{2-}$ groups with D_{2d} site symmetry in the third compound from the EPR results for Mn^{2+} in this compound alone.

Reprint requests to Dr. G. Lehmann, Institut für Physikalische Chemie, Westf. Wilhelms-Universität, Schlossplatz 4, D-4400 Münster.

Experimental

Single crystals of manganese-doped Cs_2ZnBr_4, Rb_3ZnBr_5 and $[(CH_3)_4N]_2ZnBr_4$ were grown by slow evaporation of acidified aqueous solutions of the components at 333 K. In all three cases the initial proportions of mono- and divalent ions in the solutions were 2 : 1 with 10% of the $ZnBr_2$ substituted by $MnBr_2$. Cs_3CdBr_5 was crystallized from a melt of composition $Cs_2Cd_{0.95}Mn_{0.05}Br_4$ by the Stockbarger-Bridgman method with a temperature difference between 830 and 530 K which was passed at a velocity of 2.8 cm/day. Samples of the first three compounds were analyzed for Zn and Cs_3CdBr_5 for Cd and Br. The resulting compositions agreed closely with those calculated for the pure compounds, the Mn concentrations were in all cases below 1%. Crystals suitable for EPR measurements at Q-band frequencies were selected and oriented by X-ray Weissenberg photographs using

0340-4811 / 81 / 0300-0286 $ 01.00/0. — Please order a reprint rather than making your own copy.

Mo K_α radiation. Only a thin edge of the unfavorably large crystals was exposed to the X-ray beam to reduce exposure times. The crystals grown from aqueous solutions could in many cases be oriented from their morphologies. The Q-band spectrometer used for these measurements has been previously described in detail [2]. Second order fine structure and hyperfine structure parameters were calculated using the modified computer program QCPE 69 of H. Gladney and checked by comparison with the rotation diagrams calculated with the program QCPE 68. The fourth order fine structure parameters b_4^m were not determined. The signs of b_2^0 were determined from the second order corrections of the (negative) hyperfine splitting constant A.

For the structure refinements of Cs_2ZnBr_4 (1) and Rb_3ZnBr_5 (2) single crystals with dimensions $0.39 \times 0.31 \times 0.05$) mm^3 (1) and ($0.32 \times 0.29 \times 0.21$) mm^3 (2) were selected and sealed in glass capillaries.

Precession photographs showed the expected orthorhombic symmetry and systematic extinctions compatible with the space group Pnma or its acentric counterpart $Pna2_1$ for both crystals as described by Morosin and Lingafelter [8] for (1) and Asker et al. [9] for (2). Complete sets of intensity data up to $(\sin\Theta)/\lambda = 0.64$ Å^{-1} were collected on a Syntex $P2_1$ four-circle diffractometer equipped with a molybdenum X-ray tube, graphite monochromator and scintillation counter ($\lambda_{MoK\alpha} = 0.71069$ Å, 2Θ-Θ-scan, scan speed from 3° min^{-1} to 30° min^{-1} depending on intensity, scan range 2° in 2Θ plus K_α-splitting with stationary background measurements on each side, reference reflexion every 100 reflexions) and the unit cell parameters calculated from a least squares fit of the angular settings of 15 carefully centred high order reflexions for both crystals.

The total number of unique reflexions collected for (1) is 1257 and 1482 for (2) respectively.
The crystal data are summarized as follows:

	a [Å]	b [Å]	c [Å]	SG	Z	D_x [gcm^{-3}]	μ [cm^{-1}]
Cs_2ZnBr_4	10.202(4)	7.738(3)	13.539(4)	Pnma	4	4.044	249.2
Rb_3ZnBr_5	9.079(2)	10.496(2)	13.443(3)	Pnma	4	3.740	303.7

The intensity data were corrected for absorption by an empirical procedure using the functional dependence of the intensity from the rotational setting of the diffraction vector for selected reflexions and reduced to structure amplitudes by Lorentz and polarisation corrections.

All reflexions with $I > 1.96\sigma(I)$ were accepted as observed and used in all refinement steps.

The coordinates and anisotropic thermal vibrations of the atoms in the structures of (1) and (2) were refined together with an isotropic extinction coefficient and a common scale factor by full matrix least squares methods with atomic scattering factors for neutral spherical atoms [10] taking anomalous scattering for all atoms into account. The refinements resulted in residuals of $R_1 = 0.066$ and $R_2 = 0.055$ for the 963 observed reflexions of (1) and $R_1 = 0.060$ and $R_2 = 0.049$ for the 935 observed reflexions of (2), where $R_1 = \Sigma(||F_0| - |F_c||)/\Sigma|F_0|$ and $R_2 = [\Sigma w(|F_0| - |F_c|)^2)/\Sigma w F_0^2]^{1/2}$ [11]. The weighting scheme was based on counting statistics. Tables of the calculated and observed structure factors are available from the authors.

Results

Cs_2ZnBr_4

This compound is isomorphous with Cs_2ZnCl_4 and crystallizes in the orthorhombic space group Pnma with four formula units per unit dell. Zn occupies special positions on the mirror planes. A crystal structure refinement with $R_1 = 0.114$ was reported by Morosin and Lingafelter [8] assuming isotropic temperature factors and $y = 0$ for Br(3).

The refinement of the structure with the improved data set using the published parameters [8] as starting values converged to $R_1 = 0.066$. The final positional and thermal parameters of the atoms are given in Table 1 and 2.

Table 1. Coordinates of the Atoms in the Unit Cell of Cs_2ZnBr_4.

	x	y	z
Cs (1)	0.63759 (14)	0.25	0.39664 (16)
Cs (2)	0.47640 (12)	0.25	0.82834 (11)
Zn	0.23612 (21)	0.25	0.42196 (20)
Br (1)	0.00288 (20)	0.25	0.40094 (21)
Br (2)	0.31154 (22)	0.25	0.58991 (18)
Br (3)	0.32667 (16)	− 0.00185 (22)	0.34528 (17)

Table 2. Coefficients of the Anisotropic Temperature Factors for Cs_2ZnBr_4 [x10^4][a].

	U_{11}	U_{22}	U_{33}	U_{12}	U_{13}	U_{23}
Cs(1)	387(8)	539(10)	858(16)	0	− 95(8)	0
Cs(2)	314(6)	506(9)	299(8)	0	− 10(6)	0
Zn	272(11)	330(13)	271(13)	0	7(10)	0
Br(1)	260(10)	765(18)	486(16)	0	− 73(10)	0
Br(2)	414(12)	796(18)	263(13)	0	− 96(10)	0
Br(3)	479(9)	419(10)	795(15)	− 35(7)	173(9)	− 264(10)

[a] The anisotropic temperature factors are expressed in the form
$\exp[-2\pi^2(U_{11}h^2a^{*2} + U_{22}k^2b^{*2} + U_{33}l^2c^{*2} + 2U_{12}hka^*b^* + 2U_{13}hla^*c^* + 2U_{23}klb^*c^*)]$.

Table 3.

Zn Coordination

Distances [Å]		Angles [°]	
Zn-Br(1)	2.396(3)	Br(1)-Zn-Br(2)	115.5(1)
Zn-Br(2)	2.401(4)	Br(1)-Zn-Br(3)	109.4(1)
Zn-Br(3)	2.394(2)	Br(1)-Zn-Br(3)^{I}	109.4(1)
Zn-Br(3)^{I}	2.394(2)	Br(2)-Zn-Br(3)	106.7(1)
		Br(2)-Zn-Br(3)^{I}	106.7(1)
		Br(3)-Zn-Br(3)^{I}	109.0(1)

Cs Coordination

Distances [Å]			
Cs(1)-Br(2)	4.232(3)	Cs(2)-Br(2)	3.640(3)
Cs(1)-Br(3)	3.787(2)	Cs(2)-Br(1)^{XI}	3.997(1)
Cs(1)-Br(1)^{II}	3.727(2)	Cs(2)-Br(1)^{XII}	3.675(3)
Cs(1)-Br(1)^{III}	4.257(4)	Cs(2)-Br(2)^{XII}	3.594(3)
Cs(1)-Br(2)^{IV}	3.908(1)	Cs(2)-Br(3)^{VI}	3.640(2)
Cs(1)-Br(2)^{V}	3.908(1)	Cs(2)-Br(3)^{VIII}	3.640(2)
Cs(1)-Br(3)^{VI}	4.004(3)	Cs(2)-Br(3)^{XIII}	3.647(2)
Cs(1)-Br(3)^{VII}	3.787(2)	Cs(2)-Br(3)^{XIV}	3.647(2)
Cs(1)-Br(3)^{VIII}	4.004(3)		
Cs(1)-Br(3)^{IX}	4.272(3)		
Cs(1)-Br(3)^{X}	4.272(3)		

Symmetry code:

I	$x, \frac{1}{2}-y, z$	VIII	$1-x, \frac{1}{2}+y, 1-z$
II	$1+x, y, z$	IX	$\frac{1}{2}+x, \frac{1}{2}-y, \frac{1}{2}-z$
III	$\frac{3}{2}-x, 1-y, \frac{3}{2}+z$	X	$\frac{1}{2}+x, y, \frac{1}{2}-z$
IV	$1+x, \frac{1}{2}-y, 1+z$	XI	$\frac{1}{2}-x, -\frac{1}{2}+y, \frac{1}{2}+z$
V	$1+x, \frac{3}{2}-y, 1+z$	XII	$\frac{3}{2}-x, 1-y, \frac{5}{2}+z$
VI	$1-x, -y, 1-z$	XIII	$\frac{1}{2}-x, \frac{1}{2}+y, \frac{1}{2}+z$
VII	$x, \frac{1}{2}-y, z$	XIV	$\frac{1}{2}-x, -y, \frac{1}{2}+z$

Our results differ considerably from the previous results in the distortion of the $ZnBr_4$ groups. The interatomic bond distances and angles within the $ZnBr_4$ tetrahedra and the Cs-Br distances are listed in Table 3.

The EPR fine structure and hyperfine structure data as well as the orientations of the magnetic z-axes for this and the other three compounds are collected in Table 4. The point symmetry m for Zn requires b to be one of the magnetic axes. It was found to correspond to the x-axis.

For rotation around this axis two magnetically inequivalent spectra are postulated for substitution of Zn. They were indeed observed with their z-axes deviating by $\pm 22.5°$ from the crystallographic a-axis. The superposition analysis allowed assignment of the negative sign corresponding to an angle of 15.7° between z and the Zn-Br(1) bond direction.

Rb_3ZnBr_5

This compound was found to be isomorphous with $(NH_4)_3ZnCl_5$ [9] which also has the space group Pnma with 4 formula units per unit cell [12]. The crystal structure refinement converged to $R_1 = 0.060$. The final coordinates and the coefficients of

Table 4. Summary of the EPR results.

	Cs_2ZnBr_4	Rb_3ZnBr_5	$[(CH_3)_4N]_2ZnBr_4$	Cs_3CdBr_5
$b_2^0/10^{-4}$ cm^{-1}	$+ 731.7 \pm 13.7$	$- 1279 \pm 37$	$+ 390 \pm 13$	$+ 617 \pm 28$
$b_2^2/10^{-4}$ cm^{-1}	$+ 360.8 \pm 2.2$	$- 377 \pm 40$	$+ 222 \pm 10$	0
angle between z and a-axis	− 22.5°	+ 15.0°	± 30°*	(90°)
$A_z/10^{-4}$ cm^{-1}	$- 69.8 \pm 0.2$	$- 70.9 \pm 1.0$	$- 71.0 \pm 0.5$	$- 68.6 \pm 0.5$
$A_\perp/10^{-4}$ cm^{-1}	−	−	−	$- 70.6 \pm 0.5$

* to a or c axis.

Table 5. Coordinates of the Atoms in the Unit Cell of Rb_3ZnBr_5.

	x	*y*	*z*
Rb(1)	0.41009(25)	0.25	− 0.45429(15)
Rb(2)	0.41167(19)	0.02096(16)	− 0.17149(12)
Zn	0.30926(28)	0.25	0.10877(18)
Br(1)	0.36540(30)	0.25	0.28201(17)
Br(2)	0.03550(26)	0.25	0.48588(17)
Br(3)	0.16119(26)	0.25	− 0.23414(17)
Br(4)	0.18563(20)	0.05727(15)	0.06426(13)

the anisotropic temperature factors of the atoms are given in Table 5 and 6. Table 7 contains the bond distances and angles within the $ZnBr_4$ tetrahedra and the Rb-Br coordination distances.

Thus the general pattern of the EPR spectra is the same as for Cs_2ZnBr_4, but in this case the magnetic *y*-axis coincides with the *b*-axis and the *z*-axes make angles of $\pm 15°$ with the *a*-axis. The positive sign determined from superposition analysis corresponds to an angle between *z* and the Zn-Br(2) bond direction, the longest Zn-Br bond, of 16.8° · b_2^0 is almost twice as large as in Cs_2ZnBr_4, but of opposite sign.

$(N(CH_3)_4)_2ZnBr_4$

Crystal structure data for this compound were not reported. The corresponding chloride again crystallizes in the space group Pnma [13]. We determined approximate lattice constants for the bromide of $a = 12.8$; $b = 9.3$ and $c = 16.0$ Å, their ratios agree closely with those for the chloride. Fourfold coordination of Zn (and substitutional incorporation of Mn^{2+}) follow from the green phosphorescence for Mn^{2+} with an emission maximum at 19450 cm^{-1} in close agreement with $MnBr_4^{2-}$ in other systems [14] as well as from the size of the hyperfine splitting constant *A* which is very nearly the same as for the other compounds in Table 4. The ratio $b_2^0/b_2^2 = 1.75$ is the same as for the chloride [15, 2] whereas the absolute values are four times larger in the bromide. This suggests an analogous, but presumably larger site distortion in the bromide. The magnetic *x*-axis coincides with the crystallographic *b*-axis and the *z*-axis makes angles of $\pm 30°$ with one of the other axes in the bromide. It thus appears from these EPR results that it is isomorphous with the corresponding chloride.

Cs_3CdBr_5

This compound was reported as $CdBr_2 \cdot 3CsBr$ in the phase diagram of the system CsBr–$CdBr_2$–H_2O

Table 7. Rb_3ZnBr_5.

Zn Coordination			
Distances [Å]		Angles [°]	
Zn-Br(1)	2.384(3)	Br(1)-Zn-Br(2)^{I}	109.4(1)
Zn-Br(2)^{I}	2.416(3)	Br(1)-Zn-Br(4)	110.2(1)
Zn-Br(4)	2.390(2)	Br(1)-Zn-Br(4)^{II}	110.2(1)
Zn-Br(4)^{II}	2.390(2)	Br(2)^{I}-Zn-Br(4)	105.5(1)
		Br(2)^{I}-Zn-Br(4)^{II}	105.5(1)
		Br(4)-Zn-Br(4)^{II}	115.7(1)
Rb Coordination			
Distances [Å]			
Rb(1)-Br(1)^{III}	3.568(3)	Rb(2)-Br(1)^{IX}	3.848(2)
Rb(1)-Br(2)^{III}	3.495(3)	Rb(2)-Br(1)^{X}	3.794(2)
Rb(1)-Br(3)	3.724(3)	Rb(2)-Br(2)^{IX}	3.577(2)
Rb(1)-Br(3)^{IV}	3.408(3)	Rb(2)-Br(2)^{I}	3.643(2)
Rb(1)-Br(4)^{V}	3.349(2)	Rb(2)-Br(3)	3.415(2)
Rb(1)-Br(4)^{VI}	3.349(2)	Rb(2)-Br(3)^{IV}	3.538(2)
Rb(1)-Br(4)^{VII}	3.541(3)	Rb(2)-Br(4)	3.795(2)
Rb(1)-Br(4)^{VIII}	3.541(3)	Rb(2)-Br(4)^{VI}	3.752(2)

Symmetry code:

I $\frac{3}{2} - x, 1 - y, \frac{3}{2} + z$ — VI $\frac{1}{2} - x, -y, -\frac{1}{2} + z$

II $x, \frac{1}{2} - y, z$ — VII $\frac{1}{2} + x, \frac{1}{2} - y, -\frac{1}{2} - z$

III $x, y, -1 + z$ — VIII $\frac{1}{2} + x, y, -\frac{1}{2} - z$

IV $\frac{3}{2} - x, 1 - y, \frac{1}{2} + z$ — IX $\frac{1}{2} - x, -\frac{1}{2} + y, -\frac{1}{2} + z$

V $\frac{1}{2} - x, \frac{1}{2} + y, -\frac{1}{2} + z$ — X $1 + x, \frac{1}{2} - y, z$

Table 6. Coefficients of the Anisotropic Temperature Factors for Rb_3ZnBr_5 [x 10^4][a].

	U_{11}	U_{22}	U_{33}	U_{12}	U_{13}	U_{23}
Rb(1)	314(13)	135(11)	331(13)	0	− 42(10)	0
Rb(2)	441(10)	240(9)	417(10)	50(9)	− 24(8)	53(8)
Zn	253(14)	117(13)	245(14)	0	− 12(12)	0
Br(1)	499(18)	707(21)	193(13)	0	− 49(12)	0
Br(2)	260(13)	353(15)	327(14)	0	− 76(11)	0
Br(3)	300(14)	248(10)	329(14)	0	− 6(11)	0
Br(4)	432(11)	109(7)	546(11)	− 79(7)	− 42(9)	− 18(8)

[a] The anisotropic temperature factors are expressed in the form
$\exp[-2\pi^2(U_{11}h^2a^{*2} + U_{22}k^2b^{*2} + U_{33}l^2c^{*2} + 2U_{12}hka^*b^* + 2U_{13}hla^*c^* + 2U_{23}klb^*c^*)]$.

[16] and is obviously prepared in single crystals here for the first time. It crystallizes in a tetragonal space group with $a = 6.80 \pm 0.05$ Å and $c = 7.95 \pm 0.05$ Å with $Z = 1$. It therefore cannot be isostructural with Cs_3ZnCl_5 and Cs_3ZnBr_5 with body-centered unit cells. In accordance with these crystallographic results only one EPR spectrum of axial symmetry was found for Mn^{2+}. Presence of $CdBr_4^{2-}$ is clearly indicated by the size of the hyperfine splitting constant A with an isotropic value of $-69.9 \cdot 10^{-4}$ cm^{-1}.

Superposition Analysis

In the equations

$$b_2^0 = \frac{1}{2} \sum_i (3 \cos^2 \vartheta_i - 1) \left(\frac{R_0}{R_i} \right)^{t_2} \cdot \overline{b_2} \qquad (1)$$

and

$$b_2^2 = \frac{1}{2} \sum_i \sin^2 \vartheta_i \cos 2\varphi_i \left(\frac{R_0}{R_i} \right)^{t_2} \cdot \overline{b_2} \text{ [7]} \qquad (2)$$

the constants R_0, t_2 and $\overline{b_2}$ are initially unknown. The normal M-X bond distance R for each transition metal ion — ligand combination can be taken from either the sum of the ionic radii (corrected, if necessary, for the particular coordination number) or directly from crystal structure data of pure transition metal ion compounds. $R_0 = 2.449$ Å is obtained from Cs_2MnBr_4 which is isomorphous with Cs_2ZnBr_4 [17] agreeing within less than 1% with the sum of the ionic radii. The exponent t_2 for Mn^{2+} in MgO and CaO was found to be close to 7 [3]. As shown in Fig. 1, this exponent also leads to closely agreeing values of $\overline{b_2} = +0.439 \pm 0.08$ cm^{-1} for both Rb_3ZnBr_5 and Cs_2ZnBr_4 (with our crystal structure data for the latter). The different slopes for these systems are due to dominating angular distortions in Cs_2ZnBr_4 and larger differences in bond lengths in Rb_3ZnBr_5. For $MnCl_4^{2-}$ $\overline{b_2}$ is only roughly half as large as for $MnBr_4^{2-}$ [6].

The $CdBr_4^{2-}$ units in Cs_3CdBr_5 must possess a $\bar{4}$ 2 m point symmetry (at least as long as effects of more distant atoms are neglected). Thus with the value of $\overline{b_2}$ for $MnBr_4^{2-}$ it should be possible to determine the angle between the Cd-Br bonds and the crystallographic c-axis from the sign and size of b_2^0 for Mn^{2+} in this compound if a reasonable estimate of the Cd-Br bond length R_i can be made. With the average value of 2.5805 Å for Cs_2CdBr_4

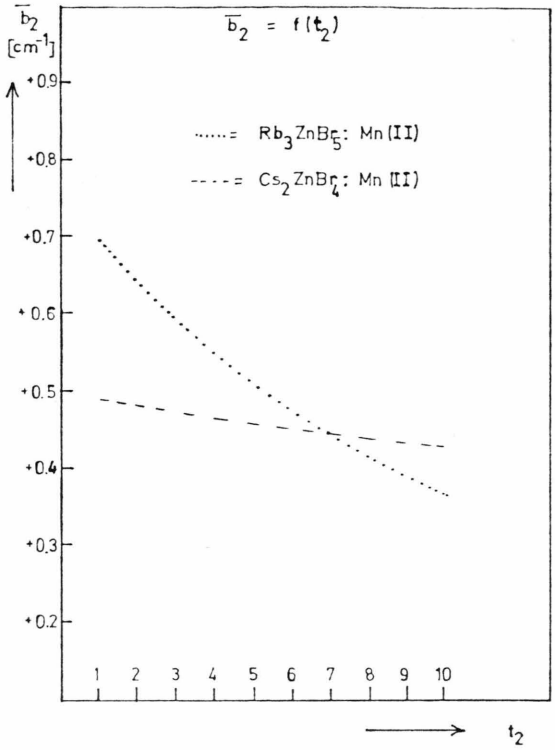

Fig. 1. Dependence of the intrinsic zero field splitting parameter $\overline{b_2}$ on the exponent t_2 for Mn^{2+} in Cs_2ZnBr_4 (our crystal structure data) and Rb_3ZnBr_5.

[18] this angle is found to be $52.9 \pm 0.2°$. Thus the $CdBr_4^{2-}$ units in Cs_3CdBr_5 are elongated along the c-axis with a bond angle of $105.7 \pm 0.4°$. This result is also in qualitative agreement with the observed anisotropy of the hyperfine splitting constant A for ^{55}Mn with larger values along directions of decreased metal — ligand overlap [19].

Discussion

The results of the superposition analyses clearly show that just like for $MnCl_4^{2-}$ [2, 6] the distortion of the first coordination sphere largely determines sign and size of the fine structure parameters as well as the directions of the magnetic axes. Within the accuracy of the crystal structure data, contributions of more distant ions as well as local lattice relaxation around the transition metal ion appear to be negligible, at least as long as the transition metal ion is incorporated in sites of diamagnetic ions of the same valence state and similar size. This offers the possibility to determine the distortions of MX_n

units with the achievable high accuracy of the EPR data, once sufficiently accurate values of $\overline{b_2}$ for the MX_n units are available. Cs_3CdBr_5 with a favorable axial site symmetry is one example for application of EPR data for the clarification of structural details of this kind; other examples are some MX_2 layer compounds with $\bar{3}$ 2/m site symmetries [20]. For low site symmetries, however, the number of variables (position parameters of ligands) always exceeds the number of available EPR parameters (sign and size of b_2^0 and b_2^2 as well as directions of magnetic axes, if not fixed by symmetry): For m site symmetry like in Cs_2ZnBr_4 and Rb_3ZnBr_5 with coordination number 4 seven degrees of freedom exist for the ligands whereas only five EPR parameters including the direction of one magnetic axis in the $a-c$ place are available; the situation is even worse for higher coordination numbers and still lower site symmetries. Thus in these cases the EPR parameters can be reproduced by more than one combination of ligand arrangements. One way to overcome this ambiguity is a comparison of the complete angular variations of measured and calculated zero field splittings. This is done for Cs_2ZnBr_4 and rotation around the b-axis in Fig. 2, where the data of both crystal structure refinements were used. In this Figure the values of ϑ_i were calculated for the whole range of orientations at sufficiently small

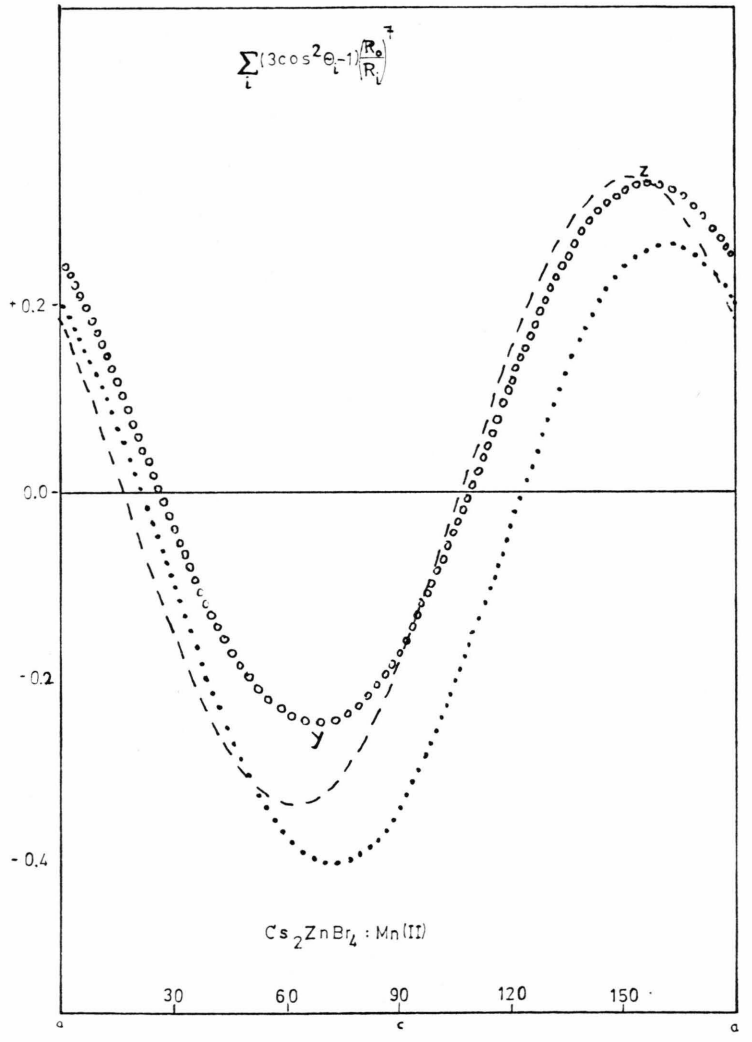

Fig. 2. Comparison of measured (○○○○) and calculated (· · · · — crystal structure data of Ref. [8]; ---- — our crystal structure data) angular variation of the zero field splitting for Mn^{2+} in Cs_2ZnBr_4 for rotation around the b (magnetic x-) axis. The measured curve is given by

$$\frac{1}{\overline{b_2}}\left[(3\cos^2\vartheta - 1)\cdot b_2^0 - \sin^2\vartheta\cdot b_2^2\right]$$

where ϑ is the angle between H_0 and the magnetic z-axis.

intervals. Clearly the positions of the magnetic axes are close to, but not exactly coinciding with the directions of extreme compression (maxima) and dilatation (minima) resulting from the crystal structure data. However, the less accurate data of Morosin and Lingafelter [8] postulate an interchange of z- and y-axes in clear contradiction to the EPR results. The deviations of measured and calculated splittings are considerably smaller for our crystal structure data, but vary with orientation. This suggests a correction of the crystal structure data (within their limits of error) for orientations of maximum deviation by shifting the positions of those ligands which have a maximum effect at these particular orientations, i.e. whose M-X bond directions are either nearly parallel or perpendicular to these directions. An attempt to obtain a perfect agreement with a shift of the Zn position in the a—c plane was unsuccessful, although the agreement was slightly improved. Such detailed comparisons are, of course, always limited by the still unknown, but certainly not completely negligible influence of more distant ions and of local lattice relaxation. On the other hand, it should at least be possible to obtain an estimate of these effects if enough correlations of this kind are available. Influences of next nearest neighbors, e.g., should manifest themselves in a tendency to coincidence of their axes directions with the orientations of maximum deviation.

The intrinsic zero field splitting parameter $\overline{b_2}$ is twice as large for $MnBr_4^{2-}$ as for $MnCl_4^{2-}$ suggesting large — direct or indirect-contributions of covalency to these zero field splittings. Additional results obtained by evaluation of data from the literature [20] also indicate a monotonic increase with covalency, but also a marked influence of coordination number. The distortion of the $ZnBr_4^{2-}$ group in $[(CH_3)_4N]_2ZnBr_4$ appears to be roughly twice as large as that of the $ZnCl_4^{2-}$ group in the corresponding chloride.

Additional information about site distortions can be obtained from the anisotropy of the hyperfine splitting constant A for ^{55}Mn (or ^{57}Fe). A regular increase with bond elongation is observed [19], and evidently angular distortions have a qualitatively similar effect, as the anisotropy for Mn^{2+} in Cs_3CdBr_5 shows. Thus a superposition analysis for the anisotropy of A should also be possible. If the exponent t_2 differs significantly from the value of 7, valid for the second order fine structure parameters, an independent additional method for evaluation of site distortions will be available. It is planned to investigate this problem more closely in the near future. Since the information in this case stems from the normally small anisotropy a high accuracy is required, and normally higher limits of error can be anticipated than for the evaluation of fine structure parameters which are directly affected by the site distortions. On the other hand, the average value of A can also give a rough indication of the average bond distance [17], an information not directly available from the fine structure data.

Acknowledgements

We thank Dr. E. Schumacher (Institut für Anorganische Chemie) for the chemical analysis of Cs_3CdBr_5 and Mrs. Hübner and Dr. P. Seidel (Institut für Mineralogie) for precession photographs of a crystal of the same compound. This work was supported by a grant from the Deutsche Forschungsgemeinschaft.

[1] P. Novák and V. Havlicek, Czech. J. Phys. **26B**, 687 (1976).
[2] H. Sachs and G. Lehmann, phys. stat. sol. (b) **92**, 417 (1979).
[3] D. J. Newman and E. Siegel, J. Phys. **C9**, 4285 (1976).
[4] E. Siegel and K. A. Müller, Phys. Rev. **B19**, 109 (1979); Phys. Rev. **B20**, 687 (1979).
[5] H. S. Murrieta, J. O. Rubio, and G. S. Aguilar, Phys. Rev. **B19**, 5523 (1979); H. S. Murrieta, F. J. Lopez, J. O. Rubio, and G. S. Aguilar, J. Phys. Soc. Japan. **49**, 499 (1980).
[6] G. Lehmann, phys. stat. sol. (b) **99**, 623 (1980).
[7] D. J. Newman, Adv. Phys. **20**, 197 (1971); D. J. Newman and W. Urban, Adv. Phys. **24**, 793 (1975).
[8] B. Morosin and E. G. Lingafelter, Acta Crystallogr. **12**, 744 (1959).
[9] W. J. Asker, D. E. Scaife, and J. A. Watts, Aust. J. Chem. **25**, 2301 (1972).
[10] "International Tables for X-ray Crystallography", Vol. IV, Kynoch Press, Birmington 1974, pp. 99 ff.
[11] The crystallographic calculations were made on a Data General Eclipse computer using, besides own programmes, the programmes of the Syntex EXTL and SHELXTL Systems.
[12] H. P. Klug and L. Alexander, J. Am. Chem. Soc. **56**, 1057 (1944).
[13] J. R. Wisner, R. C. Srivastava, C. H. L. Kennard, M. DiVaira, and E. C. Lingafelter, Acta Crystallogr. **23**, 565 (1967); B. Morosin and E. Emerson, Acta Crystallogr. **12**, 744 (1959).
[14] F. A. Cotton, D. M. L. Goodgame, and M. Goodgame, J. Amer. Chem. Soc. **84**, 167 (1962).

[15] F. D. Tsay and L. Helmholz, J. Chem. Phys. **50**, 2642 (1969).
[16] V. K. Filippov, K. A. Agafanova, and M. A. Vakinor, Zh. Neorg. Khim. **19**, 1663 (1974); V. K. Filippov and K. A. Agafanova, Zh. Prikl. Khim. Leningrad **50**, 1529 (1977); V. K. Filippov, M. A. Yakimov, V. M. Makarevskii, K. A. Agafanova, and L. P. Vivchaik, Problem. Sorrem. Khimii Koordinats. Soedin **6**, 430 (1978).
[17] J. Goodyear, G. A. Steigmann, and D. J. Kennedy, Acta Crystallogr. **B28**, 1231 (1972).
[18] D. Altermatt, H. Arend, A. Niggli, and W. Petter, Mat. Res. Bull. **14**, 1391 (1979).
[19] G. Lehmann, J. Phys. Chem. Sol. **41**, 919 (1980).
[20] M. Heming and G. Lehmann, Chem. Phys. Letters (to be published).